

Facility Location with Congestion and Priority in Drone-Based Emergency Delivery

Xin Wang

Department of Industrial Engineering, Tsinghua University, Beijing 100084, China,
Logistics and Transportation Division, Tsinghua University Shenzhen International Graduate School, Shenzhen 518055,
China, wangxin16@mails.tsinghua.edu.cn

Ruiwei Jiang

Department of Industrial and Operations Engineering, University of Michigan, Ann Arbor, Michigan, 48103, US
ruiwei@umich.edu

Mingyao Qi*

Logistics and Transportation Division, Tsinghua University Shenzhen International Graduate School, Shenzhen 518055,
China, qimy@sz.tsinghua.edu.cn

Thanks to their fast delivery, reduced traffic restrictions, and low manpower need, drones have been increasingly deployed to deliver time-critical materials, such as medication, blood, and exam kits, in emergency situations. This paper considers a facility location model of using drones as mobile servers in emergency delivery. The model jointly optimizes the location of facilities, the capacity of drones deployed at opened facilities, and the allocation of demands, with an objective of equitable response times among all demand sites. To this end, we employ queues to model the system congestion of drone requests and consider three queuing disciplines: non-priority, static priority, and dynamic priority. For each discipline, we approximate the model as a mixed-integer second-order conic program (MISOCP), which can readily be solved in commercial solvers. We conduct extensive computational experiments to demonstrate the effectiveness and accuracy of our approach. Additionally, we compare the system performance under the three queuing disciplines and various problem parameters, from which we produce operational recommendations to decision makers in emergency delivery.

Key words: Drone delivery; Facility location-allocation; Congestion; Priority queue; Mixed-integer second-order cone programming.

1. Introduction

Natural and anthropogenic disasters such as typhoons, earthquakes, terrorist attacks, and epidemic outbreaks make severe impacts on the human kind. For example, various natural disasters have caused 449k deaths and a trillion USD economic losses between 2010 and 2019 ([Ritchie 2014](#)). Additionally, as of Oct. 2021, an estimated 5 million people have

died from COVID-19 ([Max Roser and Hasell 2021](#)). Disasters trigger high demands for emergency delivery service such as medication, blood, and exam kits.

Of all characteristics in such service, response time is arguably the most significant in deciding the survival of those affected. Unfortunately, as infrastructure damages typically arrive with the disaster, traditional ground transportation often result in delay of response, especially in remote areas. In contrast, drones, or unmanned aerial vehicles, have the advantages of fast delivery, reduced traffic restrictions, and low manpower need. For example, it has been demonstrated that drones are 8 to 12 times faster than traditional methods in delivering testing sample tubes in Germany ([McNabb 2020](#)). In view of these advantages, many agencies have deployed drones to deliver small relief items (see, e.g., [BAKER \(2017\)](#) and [COMMUNITY \(25th April 2020\)](#)).

A key research task for deploying drones in emergency delivery is to optimally locate the facilities, where drones load items, and distribute drones among these facilities. To this end, several families of location models have been studied in the existing literature (see, e.g., [Jia, Ordóñez, and Dessouky \(2007\)](#)). In particular, covering models provide adequate coverage to all demand sites with a minimum number of facilities (see, e.g., [Daskin \(1983\)](#), [Marianov and Serra \(2002\)](#)), median models satisfy the demand with a minimum facility and traveling cost (see, e.g., [Berman, Larson, and Chiu \(1985\)](#), [Vidyarthi and Jayaswal \(2014\)](#)), and center models seek to improve the worst-case quality of service among all demand sites. Although the first two models have been widely applied, in this paper, we consider a center model in order to produce *equitable* response times in emergency delivery. Here, the response time for a demand request refers to the duration from when the demand arises to when it is fulfilled. As a result, the response time consists of not only the travel time of the drone but also the (random) waiting time, which occurs if there is no available drones when the demand arises due to a congestion of drone requests. We refer to [Berman and Krass \(2019\)](#) for existing studies on facility location with congestion, among which queuing is a natural and preferable modeling choice for the congestion at each opened facility. Unfortunately, it also yields a challenging facility location formulation. As a result, most existing studies adopt heuristic solution methods. In this paper, we derive an approximate solution method based on mixed-integer second-order conic programs (MISOCPs), which can readily be solved in commercial solvers.

In emergency situations, demand sites may not be equally important. For example, the epicenter of an earthquake usually suffers the largest impacts and would benefit the most from faster delivery of relief supplies. This motivates us to incorporate the following two priority disciplines into the queuing model.

- *Static priority* divides the set of demand sites into different priority levels and always fulfills the demand from a higher level before doing so to the lower ones (Silva and Serra 2008, Jayaswal and Vidyarthi 2017).

- *Dynamic priority* updates the priority of each demand site based on its inherent priority level and the waiting time it has experienced. That is, longer waiting time promotes the priority of a demand site (Jackson 1960, 1961). To our best knowledge, the dynamic priority discipline has received little attention in the facility location literature.

As a benchmark, we also consider a queuing model with no priority levels (i.e., all demand sites have the same priority). The main contributions of this paper are as follows:

1. We adopt three disciplines: non-priority, static priority, and dynamic priority to consider different emergency degrees and importance of heterogeneous demands in our facility location problem with congestion and mobile servers. To our best knowledge the dynamic priority is explored for the first time.
2. We explicitly consider the system congestion via a queuing model in a facility location problem, with an objective of equitable response times among all demand sites. We employ a generally distributed service time for drones as mobile servers, that depends on the demand assignment and facility capacity decisions.
3. We reformulate the proposed mixed-integer nonlinear programs into MISOCPs, which can be solved directly by the existing solver like Gurobi. Computational experiments are conducted for sensitivity analysis and comparison of the system performance under different priority disciplines by a hybrid approach of optimization and simulation.

The remainder of this study is organized as follows. Section 2 reviews related literature. In Sections 3–5, we consider three variants of the proposed facility location model with non-priority, static priority, and dynamic priority, respectively. In each variant, we approximate the ensuing nonlinear and non-convex model as a MISOCP. Section 6 reports the numerical results and Section 7 concludes the paper with a summary and directions for future research.

2. Literature Review

The facility location problem for emergency service has been considered in three streams of literature, namely coverage models, median models, and center models.

Coverage models seek to maximize coverage with a given number of facilities, or alternatively, cover all demands with a minimum number of facilities. In an emergency service context, probabilistic models have been considered. [Daskin \(1983\)](#) considered that more than one facility may be available when a demand request arises and proposed to maximize the probability of coverage. Alternatively, [ReVelle and Hogan \(1988\)](#) modeled the coverage probability as a constraint (i.e., chance constraint) to meet a required level of reliability. These models were later extended by [Batta, Dolan, and Krishnamurthy \(1989\)](#), [Repede and Bernardo \(1994\)](#), and [ReVelle and Hogan \(1989\)](#) to tackle other facility location problems. These models assume that the random business/idleness of all facilities are jointly independent, which may not be the case in reality. [Marianov and Revelle \(1994\)](#) and [Marianov and ReVelle \(1996\)](#) relaxed this assumption by using queues to estimate the service busy fraction around the demand node. Moreover, [Marianov and Serra \(1998\)](#) modeled each facility as an $M/M/k$ queue and explicitly imposed a constraint on waiting time or queue length to ensure the quality of service. [Marianov and Serra \(2002\)](#) later extended the same model by determining the number of servers deployed at each facility instead of giving it a priori.

Median models locate facilities to minimize the total travel time and waiting time of customers. To compute customer waiting time, [Wang, Batta, and Rump \(2002\)](#) and [Berman, Krass, and Wang \(2006\)](#) modeled each opened facility as an $M/M/1$ queue. Since this leads to a nonlinear formulation, these studies applied heuristic algorithms. A notable attempt to provide more precise solutions is from [Elhedhli \(2006\)](#), who recast the nonlinear formulation via piecewise linear approximations and proposed a cutting plane algorithm to find global optimum. Later, [Vidyarthi and Jayaswal \(2014\)](#) extended this approach to $M/G/1$ queues. More recently, [Ahmadi-Javid and Hoseinpour \(2017\)](#) recast the same model as a MISOCP and [Ahmadi-Javid and Ramshe \(2019\)](#) derived various linear reformulation of the model, as well as valid inequalities to strengthen the ensuing formulation. In addition, [Ahmadi-Javid, Berman, and Hoseinpour \(2018\)](#) modeled the service time as a function of the capacity of each facility and reformulated the nonlinear model as a MISOCP. Different from the aforementioned median models, this paper considers queues with *mobile*

servers (i.e., the drones) that travel to customers to deliver service. As a result, the service time depends not only on the waiting time in queues but also the server travel time, which further depends on which facility the demand is assigned to. For mobile servers, [Berman, Larson, and Chiu \(1985\)](#) studied a single facility with an $M/G/1$ queue. Other facility location models with a single mobile server include [Chiu, Berman, and Larson \(1985\)](#), [Berman and Mandowsky \(1986\)](#), and [Berman, Larson, and Parkan \(1987\)](#), and [Batta and Berman \(1989\)](#) extended the model to have k servers at a single facility.

Center models, which this paper employs, pay more attention to an equitable quality of service among all demand nodes than the median models. In other words, our model explicitly takes into account the equity and priority among demand nodes, which is useful in an emergency delivery context. To the best of our knowledge, center models have received limited attention in existing literature. Examples of such models include [Revelle and Hogan \(1989\)](#), who sought to minimize the maximum service time and employed chance constraints to ensure the quality of service. More recently, [Aboolian, Berman, and Drezner \(2009\)](#) modeled the congestion of facilities using an $M/M/k$ queue. They assumed the service rate of the queue to be pre-specified, while our service rates are decision-dependent.

Applications of drones in delivery service has attracted significant research attention in the recent past. Reviews of drone operational models can be found in [Otto et al. \(2018\)](#), [Macrina et al. \(2020\)](#), and [Chung, Sah, and Lee \(2020\)](#). The majority of the existing literature concentrates on routing problems, including traveling salesman problem with drones ([Murray and Chu 2015](#), [Ferrandez et al. 2016](#), [Ha et al. 2018](#), [Agatz, Bouman, and Schmidt 2018](#), [Poikonen, Golden, and Wasil 2019](#), [Salama and Srinivas 2020](#)) and vehicle routing problems with drones ([Wang, Poikonen, and Golden 2017](#), [Poikonen, Wang, and Golden 2017](#), [Daknama and Kraus 2017](#), [Wang and Sheu 2019](#), [Kitjacharoenchai, Min, and Lee 2020](#)). However, location models with drones, especially for emergency service, have received much less attention by far. [Scott and Scott \(2017\)](#) summarized the applications of drone delivery in healthcare industry. [Shavarani \(2019\)](#) studied a multi-level facility location problem considering drones, recharge stations, and relief centers without congestion. In contrast, [Boutilier and Chan \(2019\)](#) used an $M/M/k$ queue to model the congestion of a drone-based system for automated external defibrillators delivery. They also introduced a chance constraint to guarantee the service level. Our work is closely related to [Shavarani et al. \(2019\)](#), who modeled the system congestion through an $M/G/k$ queue for

each facility, analyzed the uncertain characteristics using the fuzzy theory, and provided a genetic algorithm. This paper is different from [Shavarani et al. \(2019\)](#) in three aspects: (i) we adopt a center model for equitable emergency delivery; (ii) we consider $M/G/1$ queues in the center model and derive an exact reformulation as a MISOCP; (iii) we introduce static and dynamic priorities into the queuing discipline.

Lastly, demand priorities have been addressed in emergency logistics problems, including vehicle routing (see, e.g., [Ghannadpour, Noori, and Tavakkoli-Moghaddam \(2014\)](#), [Oran et al. \(2012\)](#), and [Zhu et al. \(2019\)](#)), location routing (see, e.g., [Li, Wu, and Song \(2018\)](#)), and coverage models (see, e.g., [Silva and Serra \(2008\)](#), [Jayaswal and Vidyarthi \(2017\)](#), [Cao and Liu \(2011\)](#), [Oran et al. \(2012\)](#), and [Mukhopadhyay and Vorobeychik \(2017\)](#)). In contrast, we consider both static and dynamic priorities in a center model.

3. Non-Priority Model

We consider a facility location model with no priorities. That is, we employ a queue to model the congestion of each server and adopt the first-come-first-serve (FCFS) discipline. Specifically, we consider a set I of demand nodes and a set J of candidate facility locations (to provide relief supplies via drones). We denote by t_{ij} the travel time of a drone from demand node i to facility j . We assume that t_{ij} is known and deterministic for all (i, j) pairs. In addition, we denote by t_{max} the range of drones. That is, if the delivery time t_{ij} exceeds t_{max} , then drones from facility j do not deliver to demand node i .

Our model seeks to make three decisions: (i) x are binary variables indicating the setup of facilities, such that $x_j = 1$ if we open a facility in location j and $x_j = 0$ otherwise; (ii) y are binary variables for the assignment of demand nodes, such that $y_{ij} = 1$ if demand node i is assigned to facility j and $y_{ij} = 0$ otherwise; and (iii) k_j is an integer variable representing the number of drones deployed to facility j .

To model the system congestion, we assume that the demand at each node i is generated from a Poisson process with rate λ_i . Then, the stream of demands arriving at facility j is also Poisson with rate

$$\gamma_j = \sum_{i \in I} \lambda_i y_{ij} \tag{1}$$

for all $j \in J$. It follows that, on average, each drone at facility j spends time

$$\frac{\sum_{i \in I} \lambda_i t_{ij} y_{ij}}{\sum_{i \in I} \lambda_i y_{ij}}$$

on each delivery. As we equip each facility with k_j drones, it appears appealing to model it as an $M/G/k_j$ queue, where the service time distribution is general. Unfortunately, it is not computational viable to compute the steady-state probability of the queue [Tijms, Van Hoorn, and Federgruen \(1981\)](#) even if the decision variable k_j is pre-specified, let alone incorporating such information into an optimization model as we seek to do. In this paper, we instead adopt an $M/G/1$ queue to approximate the congestion at each facility largely because of its computational practicality [Berman and Krass \(2019\)](#), [Dan and Marcotte \(2019\)](#). As a result, the inter-service time, denoted by τ_j , has the following first and second moments:

$$\mathbb{E}[\tau_j] = \frac{\sum_{i \in I} \lambda_i t_{ij} y_{ij}}{k_j \sum_{i \in I} \lambda_i y_{ij}}, \quad (2)$$

$$\mathbb{E}[\tau_j^2] = \frac{\sum_{i \in I} \lambda_i t_{ij}^2 y_{ij}}{k_j^2 \sum_{i \in I} \lambda_i y_{ij}}. \quad (3)$$

Then, following from the Pollaczek-Khintchine formula (see, e.g., [Shortle et al. \(2018\)](#)), the expected waiting time of the queue at facility j equals

$$W_j = \frac{\gamma_j \mathbb{E}[\tau_j^2]}{2(1 - \gamma_j \mathbb{E}[\tau_j^2])},$$

which is re-written in terms of our decision variables

$$W_j = \frac{\sum_{i \in I} \lambda_i t_{ij}^2 y_{ij}}{2k_j(k_j - \sum_{i \in I} \lambda_i t_{ij} y_{ij})}. \quad (4)$$

We are now ready to present our model without priority as follows.

$$\text{(NP)} \quad \min_{x, y, k} \quad \max_{i \in I, j \in J} \{t_{ij} y_{ij} + W_j\} \quad (5a)$$

$$\text{s.t.} \quad \sum_{j \in J} y_{ij} = 1 \quad \forall i \in I, \quad (5b)$$

$$y_{ij} \leq x_j \quad \forall i \in I, \forall j \in J, \quad (5c)$$

$$\sum_{j \in J} y_{ij} t_{ij} \leq t_{max} \quad \forall i \in I, \quad (5d)$$

$$\sum_{i \in I} \lambda_i t_{ij} y_{ij} \leq k_j \quad \forall j \in J, \quad (5e)$$

$$\sum_{j \in J} k_j \leq K \quad (5f)$$

$$x_j, y_{ij} \in \{0, 1\}, \quad k_j \in \mathbb{Z}_+, \quad \forall i \in I, \forall j \in J. \quad (5g)$$

The objective function (5a) minimizes the longest expected response time, which is the expected waiting time plus the travel time of the drone, among all demand nodes. Constraints (5b)–(5d) ensure that each demand node is assigned to a facility that is open and within the range of drones. Constraints (5e) ensure that the queue at each facility is stable. Finally, Constraints (5f) cap the number of drones we can deploy at opened facilities. The parameter K can be decided, for example, by pre-solving a side optimization model that seeks the minimum number of drones to maintain the stability of all queues, i.e., $\min_{x,y,k} \{\sum_{j \in J} k_j : (5b)–(5e), (5g)\}$. Then, we can set K to be $(1 + \alpha)$ times of the minimum number of drones thus obtained, where $\alpha \geq 0$ can be specified by a planner depending on resource abundance.

The objective function of model (NP), particularly the waiting time W_j defined in (4), appears to be nonlinear and nonconvex. As a consequence, (NP) cannot be solved by off-the-shelf optimization solvers (e.g., Gurobi) and raises a concern of computational intractability. In the following theorem, we show that the epigraph of W_j as a function of k_j and y_{ij} admits a second-order conic representation. This produces a MISOCP reformulation of (NP), which can directly be computed by optimization solvers.

THEOREM 1. *The optimal value and the set of optimal solutions of model (NP) coincide with those of the following MISOCP:*

$$\min Z_{max} \tag{6a}$$

$$s.t. Z_{max} \geq t_{ij}y_{ij} + W_j \quad \forall i \in I, \forall j \in J, \tag{6b}$$

$$\left\| \begin{array}{c} \sqrt{2\lambda_1}t_{1j}\theta_{1j} \\ \vdots \\ \sqrt{2\lambda_I}t_{Ij}\theta_{Ij} \end{array} \right\| \leq k_j - \sum_{i \in I} \lambda_i t_{ij} y_{ij} + W_j \quad \forall j \in J, \tag{6c}$$

$$\left\| \begin{array}{c} 2y_{ij} \\ \theta_{ij} - \beta_{ij} \end{array} \right\|_2 \leq \theta_{ij} + \beta_{ij} \quad \forall i \in I, j \in J, \tag{6d}$$

$$\left\| \begin{array}{c} 2\beta_{ij} \\ 1 - k_j \end{array} \right\|_2 \leq 1 + k_j \quad \forall i \in I, j \in J, \tag{6e}$$

$$(5b)–(5g). \tag{6f}$$

Proof of Theorem 1. We start by rewriting the objective function (5a) in the epigraphic form of $\min\{Z_{\max} : Z_{\max} \geq t_{ij}y_{ij} + W_j, \text{ for all } i \in I, j \in J\}$. Accordingly, we can rewrite the definition of W_j in (4) in the epigraphic form without loss of optimality:

$$W_j \geq \frac{\sum_{i \in I} \lambda_i t_{ij}^2 y_{ij}}{2k_j(k_j - \sum_{i \in I} \lambda_i t_{ij} y_{ij})}.$$

In what follows, we assume that $k_j > 0$ and $k_j - \sum_{i \in I} \lambda_i t_{ij} y_{ij} > 0$ and the result will remain valid when either of them equals zero. Then, multiplying both sides of the above inequality by $4(k_j - \sum_{i \in I} \lambda_i t_{ij} y_{ij})$ yields that there exist $\theta_{ij} \geq 0$ for all $i \in I$ with

$$4W_j \left(k_j - \sum_{i \in I} \lambda_i t_{ij} y_{ij} \right) \geq 2 \sum_{i \in I} \lambda_i t_{ij}^2 \theta_{ij}^2, \quad (7)$$

$$\theta_{ij}^2 \geq \frac{y_{ij}}{k_j} \quad \forall i \in I. \quad (8)$$

Next, we recast (7) and (8) separately. For (7), it holds that

$$\begin{aligned} (7) &\iff \left(k_j - \sum_{i \in I} \lambda_i t_{ij} y_{ij} + W_j \right)^2 \geq 2 \sum_{i \in I} \lambda_i t_{ij}^2 \theta_{ij}^2 + \left(k_j - \sum_{i \in I} \lambda_i t_{ij} y_{ij} - W_j \right)^2 \\ &\iff (6c). \end{aligned}$$

For (8), we use the fact that $y_{ij}^4 = y_{ij}$ since y_{ij} is binary, and it holds that

$$(8) \iff \exists \beta_{ij} \geq 0 : \begin{cases} y_{ij} \leq \sqrt{\theta_{ij} \beta_{ij}} \\ \beta_{ij} \leq \sqrt{k_j} \end{cases} \quad \forall i \in I.$$

Then, following a similar procedure for recasting (7), we arrive at the representation (6d)–(6e) of (8). This completes the proof. \square

4. Static Priority Model

In emergency delivery (e.g., after a natural disaster), the degrees of importance and urgency of supplies are highly heterogeneous. Materials that involve risks to human life, such as first-aid supplies and medications, may deserve higher priority over other materials like water and food. For example, China divides the emergency relief supplies into 3 major categories and 65 minor categories (NDR 2015).

This section extends the (NP) model to consider priorities among demands with different categories. Specifically, we categorize the demand requests into R priority classes and a

smaller index represents a higher priority. Note that this categorization only depends on the types of demand requests and not on time. Accordingly, we call the priority *static* and shall generalize it to dynamic priority in Section 5. For each demand node $i \in I$, we denote by v_{ir} the probability of the node requesting a class- r demand with $\sum_{r \in R} v_{ir} = 1$. Additionally, we allow to assign the demands from different classes to different facilities and extend the decision variables y_{ij} to be y_{ij}^r , such that $y_{ij}^r = 1$ if we assign demands in class r to facility j and $y_{ij}^r = 0$ otherwise. Then, the arrival rate of the demands in class r at facility j becomes

$$\gamma_{jr} = \sum_{i \in I} \lambda_i v_{ir} y_{ij}^r \quad (9)$$

for all $j \in J$. At each opened facility j , we consider a non-preemptive priority queue. That is, the queue dynamically maintains a list of demand requests in the order of their priorities and uses their arriving times as the tie breaker. Whenever a drone becomes available, it fulfills the top-ranked request. However, a drone does not interrupt (i.e., preempt) an ongoing delivery for a new request, even if the request has higher priority than what is being delivered. This is reasonable because otherwise drones would spend a significant portion of its time traveling for nothing. It follows that the inter-service time τ_{jr} of demands in class r has the following first and second moments:

$$E[\tau_{jr}] = \frac{\sum_{i \in I} \lambda_i v_{ir} t_{ij} y_{ij}^r}{k_j \sum_{i \in I} \lambda_i v_{ir} y_{ij}^r}, \quad (10)$$

$$E[\tau_{jr}^2] = \frac{\sum_{i \in I} \lambda_i v_{ir} t_{ij}^2 y_{ij}^r}{k_j^2 \sum_{i \in I} \lambda_i v_{ir} y_{ij}^r}. \quad (11)$$

Then, the expected waiting time W_{jr} of class- r demand at facility j follows from existing results of $M/G/1$ queues with static, non-preemptive priority discipline (see, e.g., [Shurtle et al. \(2018, Ch. 4.4\)](#))

$$W_{j1} = \frac{\sum_{\ell=1}^R \gamma_{j\ell} \mathbb{E}[\tau_{j\ell}^2]}{2(1 - \gamma_{j1} \mathbb{E}[\tau_{j1}])},$$

$$W_{jr} = \frac{\sum_{\ell=1}^R \gamma_{j\ell} \mathbb{E}[\tau_{j\ell}^2]}{(1 - \sum_{\ell=1}^r \gamma_{j\ell} \mathbb{E}[\tau_{j\ell}]) (1 - \sum_{\ell=1}^{r-1} \gamma_{j\ell} \mathbb{E}[\tau_{j\ell}])} \quad \forall r \geq 2.$$

Re-writing these formulae in terms of our decision variables yields

$$W_{j1} = \frac{\sum_{\ell=1}^R \sum_{i \in I} \lambda_i v_{i\ell} t_{ij}^2 y_{ij}^\ell}{2k_j (k_j - \sum_{i \in I} \lambda_i v_{i1} t_{ij} y_{ij}^1)}, \quad (12)$$

$$W_{jr} = \frac{\sum_{\ell=1}^R \sum_{i \in I} \lambda_i v_{i\ell} t_{ij}^2 y_{ij}^\ell}{2(k_j - \sum_{\ell=1}^r \sum_{i \in I} \lambda_i v_{i\ell} t_{ij} y_{ij}^\ell) (k_j - \sum_{\ell=1}^{r-1} \sum_{i \in I} \lambda_i v_{i\ell} t_{ij} y_{ij}^\ell)} \quad \forall r \geq 2. \quad (13)$$

This produces the following extension of model (NP) based on static priority:

$$(\mathbf{SP}) \quad \min_{x,y,k} \sum_{r=1}^R w_r \max_{i \in I, j \in J} \{t_{ij} y_{ij}^r + W_{jr}\} \quad (14a)$$

$$\text{s.t.} \quad \sum_{j \in J} y_{ij}^r = 1 \quad \forall i \in I, \forall r \in [R], \quad (14b)$$

$$y_{ij}^r \leq x_j \quad \forall i \in I, \forall j \in J, \forall r \in [R], \quad (14c)$$

$$\sum_{j \in J} y_{ij}^r t_{ij} \leq t_{max} \quad \forall i \in I, \forall r \in [R], \quad (14d)$$

$$\sum_{r=1}^R \sum_{i \in I} \lambda_i t_{ij} y_{ij} \leq k_j \quad \forall j \in J, \quad (14e)$$

$$\sum_{j \in J} k_j \leq K \quad (14f)$$

$$x_j, y_{ij}^r \in \{0, 1\}, \quad k_j \in \mathbb{Z}_+, \quad \forall i \in I, \forall j \in J, \forall r \in [R]. \quad (14g)$$

In model (SP), a planner uses a weight w_r to indicate the relative importance of the worst-case response time of class- r demand requests, with $\sum_{r=1}^R w_r = 1$ and each $w_r \geq 0$. In addition, like in model (NP), the cap number K of drones can be decided, e.g., by pre-solving a side model that seeks the minimum number of drones to maintain the stability of all queues.

As evidenced in the definitions (12)–(13), (SP) involves an even higher degree of non-linearity than (NP). Nevertheless, the following theorem shows that (SP) still admits a MISOCP representation and can be computed directly by an off-the-shelf solver.

THEOREM 2. *The optimal value and the set of optimal solutions of model (SP) coincide with those of the following MISOCP:*

$$\min \sum_{r=1}^R w_r Z_r \quad (15a)$$

$$\text{s.t.} \quad Z_r \geq t_{ij} y_{ij}^r + W_{jr} \quad \forall i \in I, \forall j \in J, \forall r \in [R], \quad (15b)$$

$$\left\| \begin{array}{c} \sqrt{2\lambda_1 v_{11}} t_{1j} \theta_{1j}^\ell \\ \vdots \\ \sqrt{2\lambda_I v_{IR}} t_{Ij} \theta_{Ij}^R \\ k_j - \sum_{r=1}^R \sum_{i \in I} \lambda_i v_{il} t_{ij} y_{ij}^\ell - W_{jr} \end{array} \right\|_2 \leq k_j - \sum_{r=1}^R \sum_{i \in I} \lambda_i v_{il} t_{ij} y_{ij}^\ell + W_{jr} \quad \forall j \in J, \quad (15c)$$

$$\left\| \begin{array}{c} 2y_{ij}^\ell \\ \theta_{ij}^\ell - \beta_{ij}^\ell \end{array} \right\|_2 \leq \theta_{ij}^\ell + \beta_{ij}^\ell \quad \forall i \in I, \forall j \in J, \forall r \in [R], \quad (15d)$$

$$\left\| \begin{array}{c} 2\beta_{ij}^\ell \\ 1 - k_j + \sum_{\ell=1}^{r-1} \sum_{i \in I} \lambda_i v_{i\ell} t_{ij} y_{ij}^\ell \end{array} \right\|_2 \leq 1 + k_j - \sum_{\ell=1}^{r-1} \sum_{i \in I} \lambda_i v_{i\ell} t_{ij} y_{ij}^\ell \quad \forall i \in I, \forall j \in J, \forall r \in [R], \quad (15e)$$

$$(14b)-(14g). \quad (15f)$$

Proof of Theorem 2. We start by rewriting the objective function of (SP) in the epigraphic form of $\min\{\sum_{r=1}^R w_r Z_r : Z_r \geq t_{ij} y_{ij}^r + W_{jr}, \text{ for all } i \in I, j \in J, r \in [R]\}$. In what follows, we represent the definition of W_{jr} , as a function of decision variables k_j and y_{ij}^ℓ shown in (13), as second-order conic constraints. The representation of (12) is similar and omitted. To this end, we rewrite (13) in its epigraphic form without loss of optimality:

$$W_{jr} \geq \frac{\sum_{\ell=1}^R \sum_{i \in I} \lambda_i v_{i\ell} t_{ij}^2 y_{ij}^\ell}{2(k_j - \sum_{\ell=1}^r \sum_{i \in I} \lambda_i v_{i\ell} t_{ij} y_{ij}^\ell)(k_j - \sum_{\ell=1}^{r-1} \sum_{i \in I} \lambda_i v_{i\ell} t_{ij} y_{ij}^\ell)}.$$

This inequality holds if and only if there exist $\theta_{ij}^\ell \geq 0$ for all $\ell \in [R]$ and $i \in I$ such that

$$2W_{jr} \left(k_j - \sum_{\ell=1}^r \sum_{i \in I} \lambda_i v_{i\ell} t_{ij} y_{ij}^\ell \right) \geq \sum_{\ell=1}^R \sum_{i \in I} \lambda_i v_{i\ell} t_{ij}^2 (\theta_{ij}^\ell)^2, \quad (16a)$$

$$(\theta_{ij}^\ell)^2 \geq \frac{y_{ij}^\ell}{k_j - \sum_{\ell=1}^{r-1} \sum_{i \in I} \lambda_i v_{i\ell} t_{ij} y_{ij}^\ell} \quad \forall i \in I, \forall r \in [R]. \quad (16b)$$

We recast (16a) and (16b) separately. For (16a), it holds that

$$\begin{aligned} & (16a) \\ \iff & \left(k_j - \sum_{\ell=1}^r \sum_{i \in I} \lambda_i v_{i\ell} t_{ij} y_{ij}^\ell + W_{jr} \right)^2 \geq 2 \sum_{\ell=1}^R \sum_{i \in I} \lambda_i v_{i\ell} t_{ij}^2 (\theta_{ij}^\ell)^2 + \left(k_j - \sum_{\ell=1}^r \sum_{i \in I} \lambda_i v_{i\ell} t_{ij} y_{ij}^\ell - W_{jr} \right)^2 \\ \iff & (15c). \end{aligned}$$

For (16b), we use the fact that $(y_{ij}^\ell)^4 = y_{ij}^\ell$ since y_{ij}^ℓ is binary, and it holds that

$$(16b) \iff \exists \beta_{ij}^\ell \geq 0: \begin{cases} y_{ij}^\ell \leq \sqrt{\theta_{ij}^\ell \beta_{ij}^\ell} \\ \beta_{ij}^\ell \leq \sqrt{k_j - \sum_{\ell=1}^{r-1} \sum_{i \in I} \lambda_i v_{i\ell} t_{ij} y_{ij}^\ell} \end{cases} \quad \forall i \in I, \forall r \in [R].$$

Then, following a similar procedure for recasting (16a), we arrive at the representation (15d)–(15e) of (16b). This completes the proof. \square

5. Dynamic Priority Model

5.1. Preliminaries

In static-priority disciplines, the priority value of a demand is a fixed inherent quality independent of time. However, in some practical situations the priority value of a demand point is determined not only by its class, but also the time it has spent in the queue.

[Jackson \(1960\)](#) first studied the dynamic non-preemptive priority discipline and assumed priority function at time t of the following form:

$$q_r(t) = a_r + (t - T_r) \quad t > T_r, \quad (17)$$

with geometrically distributed interarrival and service time. In this function, parameter a_r denotes the initial priority value and T_r is the arrival time of a class r customer. The server selects the next customer with the highest instantaneous priority value of $q_r(t)$.

[Bagchi and Sullivan \(1985\)](#) dealt with another form, where the priority function is given by

$$\begin{aligned} q_r(t) &= a_r + b_r(t - T_r) \quad t \geq T_r, \\ 0 < b_1 &\leq b_2 \leq \dots \leq b_r, \\ a_1 &> a_2 > \dots > a_p, \end{aligned} \quad (18)$$

based on the queuing system with Poisson arrival patterns and general service time. They derived an expression for the expected waiting time of each class of customers with different priorities, and the bounds of this expression were also given.

In our problem, we choose to use the priority function of [Jackson \(1960\)](#), which is a special case of (18) when

$$b_1 = b_2 = \dots = b_r = 1.$$

Therefore, the upper bounds of expected waiting time of each class can be finally computed as ([Bagchi and Sullivan 1985](#))

$$\overline{W}_r = W_0 + \sum_{i=1}^{r-1} \rho \rho_i \Delta a_{ir} \quad \forall j \in J, \forall r \in R, \quad (19)$$

where

$$\Delta a_{ir} = a_i - a_r. \quad (20)$$

Δa_{ir} indicates the initial priority-class gap between class i and r , and W_0 denotes the expected waiting time in the $M/G/1$ queuing system without special priority disciplines. ρ is the total utilization of the queuing system, and ρ_i is the utilization of class i customers.

5.2. Model

In a real-life situation, given the occurrence of a sudden disaster, the priorities of the affected areas can be assessed by an evaluation index system (Tian 2016), according to the estimated extent of damage, population density, economic level, and other indexes associated with these areas. Although it is important to reduce the response time of high priority areas, the demand from lower priority areas should not wait endlessly after the high priorities. Different from the static priority problem, we consider dynamic priority for the area priority problem instead.

We now define the notation specific to this model. The priority class of each demand node is given. Let $I_r \in I$ denote the set of all demand nodes with priority r . We adopt (17) as the priority value function with $a_1 > a_2 > \dots > a_r$. When there is an available drone looking for a new demand to deliver, the one with the highest priority value will be selected. The fraction that the drone is busy at facility j with priority r demand takes the value

$$\rho_{jr} = \frac{\sum_{i \in I_r} \lambda_i t_{ij} y_{ij}}{k_j} \quad \forall j \in J, \forall r \in R,$$

satisfying $\rho_j = \sum_{r \in R} \rho_{jr}$.

The expected waiting time of a demand in an $M/G/1$ system under a FCFS discipline at server j is denoted by W_j , which has been given by formula (4) and further transformed into (8)~(6e). Since there is no simple closed-form expression of the expected waiting time of demands with all priorities, the upper bounds are used in our problem. This kind of approach is reasonable, because our objective is to minimize the weighted maximum response time, where the real value will not exceed the value obtained by the upper bounds from our model. Then the expected waiting time at facility j under dynamic priority discipline is approximated as

$$\begin{aligned} W_{j1} &= W_j \quad \forall j \in J, \\ W_{jr} &= W_j + \sum_{i=1}^{r-1} \rho_j \rho_{jr} \Delta a_{ir} \quad \forall j \in J, \forall r \geq 2 \end{aligned} \quad (21)$$

By substituting our decision variables, we obtain

$$W_{jr} = W_j + \sum_{l=1}^{r-1} \Delta a_{lr} \frac{(\sum_{i \in I_l} \lambda_i t_{ij} y_{ij}) (\sum_{i \in I_l} \lambda_i t_{ij} y_{ij})}{k_j^2} \quad \forall j \in J, \forall r \geq 2. \quad (22)$$

Similar to the (NP) model, we show the following extension of model based on dynamic priority:

$$\text{(DP)} \quad \min_{x,y,k} \sum_{r=1}^R w_r \max_{i \in I_r, j \in J} \{t_{ij}y_{ij} + W_{jr}\} \quad (23a)$$

$$\text{s.t. (5b)–(5g).} \quad (23b)$$

The weight w_r indicating the relative importance of the worst-case response time of class- r demand requests, still should satisfy $\sum_{r=1}^R w_r = 1$ and each $w_r \geq 0$. In addition, like in model (NP), the cap number K of drones can be decided, e.g., by pre-solving a side model that seeks the minimum number of drones to maintain the stability of all queues.

Due to the complexity of equations (22), (DP) involves an even higher degree of non-linearity than (NP) and (SP). Nevertheless, the following theorem shows that (DP) still admits a MISOCP representation and can be computed directly by an off-the-shelf solver.

THEOREM 3. *The optimal value and the set of optimal solutions of model (DP) coincide with those of the following MISOCP:*

$$\min \sum_{r=1}^R w_r Z_r \quad (24a)$$

$$\text{s.t. } Z_r \geq t_{ij}y_{ij} + W_{jr} \quad \forall r \in [R], \forall i \in I_r, \forall j \in J, \quad (24b)$$

$$W_{jr} = W_j + \sum_{l=1}^r \Delta a_{lr} Q_{jl} \quad \forall j \in J, \forall r \geq 2, \quad (24c)$$

$$\left\| \begin{array}{c} 2\pi_{11jr} \\ \vdots \\ 2\pi_{II_r jr} \\ Q_{jr} - k_j \end{array} \right\| \leq Q_{jr} + k_j \quad \forall j \in J, \forall r \in [R], \quad (24d)$$

$$\left\| \begin{array}{c} 2y_{ij} \\ p_{iljr} - \pi_{iljr} \end{array} \right\| \leq p_{iljr} + \pi_{iljr} + 2(1 - y_{lj}) \quad \forall i \in I, \forall \ell \in I_r, \forall j \in J, \forall r \in [R], \quad (24e)$$

$$\left\| \begin{array}{c} 2p_{iljr} \\ k_j - \frac{1}{h_{iljr}} y_{lj} \end{array} \right\| \leq k_j + \frac{1}{h_{iljr}} y_{lj} \quad \forall i \in I, \forall \ell \in I_r, \forall j \in J, \forall r \in [R], \quad (24f)$$

$$(6c)–(6f), (21). \quad (24g)$$

Proof of Theorem 3. We start by rewriting the objective function of (DP) in the epigraphic form of $\min\{\sum_{r=1}^R w_r Z_r : Z_r \geq t_{ij}y_{ij} + W_{jr}, \text{ for all } r \in [R], i \in I_r, j \in J\}$. In what

follows, we represent the definition of $W_{jr}(r \geq 2)$ in formula (22) as a function of decision variables k_j and y_{ij} shown in (13), as second-order conic constraints. We introduce an auxiliary variable

$$Q_{jr} = \frac{(\sum_{i \in I} \lambda_i t_{ij} y_{ij}) (\sum_{i \in I_r} \lambda_i t_{ij} y_{ij})}{k_j^2} \quad \forall j \in J, \forall r \in [R]. \quad (25)$$

Without loss of optimality, we rewrite this equation in its epigraphic form, and obtain

$$(22) \iff : \begin{cases} (24c), \\ Q_{jr} \geq \frac{(\sum_{i \in I} \lambda_i t_{ij} y_{ij}) (\sum_{i \in I_r} \lambda_i t_{ij} y_{ij})}{k_j^2} \quad \forall j \in J, \forall r \in [R], \end{cases}$$

$$\iff : \begin{cases} (24c), \\ Q_{jr} k_j \geq \sum_{i \in I} \sum_{\ell \in I_r} \left(\frac{\lambda_i \lambda_\ell t_{ij} t_{\ell j} y_{ij} y_{\ell j}}{k_j} \right) \quad \forall j \in J, \forall r \in [R]. \end{cases} \quad (26)$$

Next, we give the procedure to recast (26) as a MISOCP. Let $h_{i\ell jr} = \lambda_i \lambda_\ell t_{ij} t_{\ell j}$, the inequality (26) holds if and only if there exists $\pi_{i\ell jr} \geq 0$, for all $r \in [R], \ell \in I_r, i \in I$ and $j \in J$, such that

$$Q_{jr} k_j \geq \sum_{i \in I} \sum_{\ell \in I_r} \pi_{i\ell jr}^2 \quad \forall i \in I, \forall \ell \in I_r, \forall j \in J, \forall r \in [R], \quad (27)$$

$$\pi_{i\ell jr}^2 \geq \frac{h_{i\ell jr} y_{ij} y_{\ell j}}{k_j} \quad \forall i \in I, \forall \ell \in I_r, \forall j \in J, \forall r \in [R]. \quad (28)$$

Then (27) is easy to be reformulated to SOC constraints (24d). We now prove that so is inequality (28). Indeed, if $y_{\ell j} = 1$ then (28) can be re-written as

$$y_{ij} \leq \left(\frac{1}{h_{i\ell jr}} \pi_{i\ell jr}^2 k_j \right)^{1/4} \quad \forall i \in I, \forall \ell \in I_r, \forall j \in J, \forall r \in [R].$$

This inequality holds if and only if there exists an $p_{i\ell jr} \geq 0$ such that

$$(2y_{ij})^2 \leq (p_{i\ell jr} + \pi_{i\ell jr})^2 - (p_{i\ell jr} - \pi_{i\ell jr})^2 \quad \forall i \in I, \forall \ell \in I_r, \forall j \in J, \forall r \in [R],$$

$$(2p_{i\ell jr})^2 \leq \left(k_j + \frac{1}{h_{i\ell jr}} \right)^2 - \left(k_j - \frac{1}{h_{i\ell jr}} \right)^2 \quad \forall i \in I, \forall \ell \in I_r, \forall j \in J, \forall r \in [R].$$

It remains to incorporate the case that $y_{\ell j} = 0$. To this end, we revise the above two inequalities as

$$(2y_{ij})^2 \leq (p_{i\ell jr} + \pi_{i\ell jr} + 2(1 - y_{\ell j}))^2 - (p_{i\ell jr} - \pi_{i\ell jr})^2 \quad \forall i \in I, \forall \ell \in I_r, \forall j \in J, \forall r \in [R],$$

$$(2p_{i\ell jr})^2 \leq \left(k_j + \frac{1}{h_{i\ell jr}} y_{\ell j} \right)^2 - \left(k_j - \frac{1}{h_{i\ell jr}} y_{\ell j} \right)^2 \quad \forall i \in I, \forall \ell \in I_r, \forall j \in J, \forall r \in [R].$$

both of which are second-order conic representable. The corresponding standard-form SOC constraints are (24e)–(24f). This completes the proof. \square

6. Computational study

In this section, we conduct the computational study to analyze the performance of the proposed location-allocation problems with congestion under non-priority, static priority, and dynamic priority disciplines. Since $M/G/1$ queuing system is applied to approximate $M/G/k$ queue, we use the simulation method to evaluate the system performance. This approach combines optimization model and simulation, which has been used in several studies (Fujiwara, Makjamroen, and Gupta 1987, Goldberg et al. 1990, Harewood 2002). Our research builds the simulators of the $M/G/k$ queuing system based on the three disciplines respectively. The simulators are built in the SimPy with Python. The optimal solutions of the mathematical programming models together with other initial settings are input in the simulators. The total running time of each simulation process is set to be 30,000 time units to ensure the stable state of the queuing system. Then the average waiting time of each priority class at each center obtained from the simulation together with the travel time is used to analyze the performance.

In section 6.1, we investigate the impact of the number of drones and the weight of priorities on response time of the static priority problem and compare the performance between the non-priority and static priority system. In section 6.2, sensitivity analysis is conducted for the dynamic priority problem. The performance of the system is compared to that of static priority and non-priority system.

The deduced SOCP formulations are solved by Gurobi Optimizer version 9.0.1. All tests are performed on a personal computer with 2.9 GHz processor and 8 GB memory, running Windows 10 operating system. In all non-priority, static priority and dynamic priority problems, the coordinates of both the candidate facilities and demand nodes are randomly generated in a uniform distribution $U(0, 30)$. Drone speed is set to 80 km/h, and its endurance is 40 min. The default value of w_1 is set to 70%.

6.1. Analysis of static priority problem

This section gives the computational results of our facility location-allocation problem with congestion and static priority. We explore the impacts of different coefficients on the performance of the system, and evaluate the gap between non-priority and static priority systems by comparing response time and waiting time to the non-priority system.

In all experiments, we use the instances comprised of 10 demand nodes with 2 priority classes of materials at any node and 6 candidate service centers. The average arrival rate

at demand node i is randomly generated as $\lambda_i \sim U(0.6, 1)$. The proportion for demands of priority class 1 of each node v_{i1} is produced by the uniform distribution of $(0, 1)$, leading to $v_{i2} = 1 - v_{i1}$. The initial maximum total number of drones is set to 200.

6.1.1. Impact of the number of drones

In this section, we investigate the impact of the number of drones on response time in the static priority system. Based on the aforementioned settings, we first solve the side model to get the minimum number of drones K^* associated with the stable queuing system. Then we run a set of experiments for (SP) using different values of α (0, 0.02, 0.05, 0.1, 0.2, 0.5, 1) to bound the total number of drones, taking the value of $K^*(1 + \alpha)$. For each of the above settings, we can obtain the optimal decision of the location of the open centers, the allocation of the demands, and the deployment of the drones, all of which are further input into the simulator to access the system performance.

We select a typical instance to represent the results of both the optimization model and the simulation in Figure 1. The weighted expected response time Z which is the objective function of (SP) goes down as the number of drones increases in both situations. The values obtained from the optimization model are a little higher than the simulation results, but the difference is not that pronounced. The weighted response time is extremely high when α is very small, and shows a sharp decrease as α rises. Finally, it becomes stable when α exceeds 0.2. The observation is associated with the fact that when drones are particularly scarce, the waiting time of demands takes a large portion in the response time. However, when drones become sufficient, the waiting time becomes really small even to 0 while the travel time achieves the dominant role instead, leading to the stabilization of Z . The results suggest the unnecessary to distribute excessive drones at the centers which stands for a high cost. According to our experiments on majority instances, setting α around 0.2 can decrease the response time significantly without incurring too much cost.

To analyze the impact of drone number on each priority class, Figure 2 provides the results for 10 randomly generated instances under each value of α . Without specific denoting, the results are obtained through the optimization-simulation approach. Z_r is the maximum expected response time among all demand nodes with priority r . The mean value of all instances is shown as the middle line in the area between the upper and lower quartiles. The variation trend of class 2 demand is similar to that of Z , which declines dramatically at first and becomes stable later on. However, there is only a slight decrease in class 1

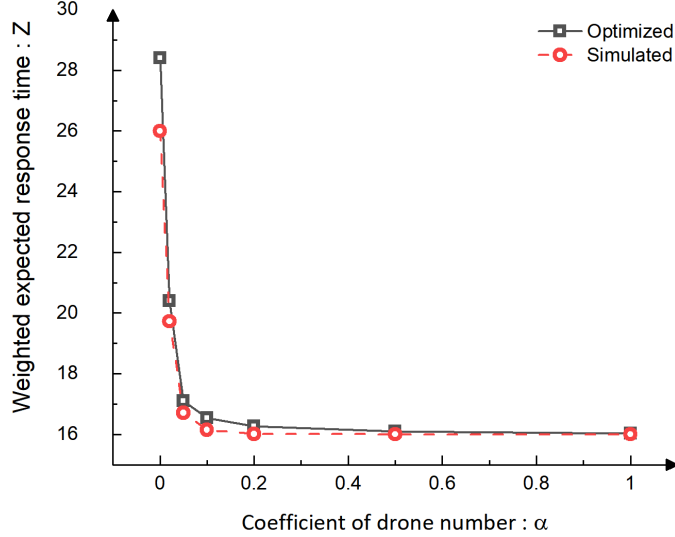


Figure 1 Weighted expected response time Z under different α (0, 0.02, 0.05, 0.1, 0.2, 0.5, 1)

demand throughout. The reason is that in the static priority queuing system, the demands from class 1 have strict priority over the others. Once there is an available drone, the highest priority demand will be delivered immediately, even the relatively small number of drones doesn't have a big influence. However, when drones are insufficient, it will take a long time to deliver all existing and successively emerging demands of class 1 before a drone is able to serve a class 2 demand. Besides, it is noted that the maximum response time of class 2 is always larger than that of class 1 and finally becomes equal when drones are sufficient.

6.1.2. Impact of the weight coefficients

In this section, we study the impact of the weight of priorities w_r on system performance. In addition to the maximum response time Z_r , we also evaluate the performance of total response time $sumZ_r = \sum_{i \in I_r} \lambda_i v_{ir} y_{ij}^r (t_{ij} + W_{jr})$, maximum waiting time W_r , and total waiting time $sumW_r = \sum_{i \in I_r} \lambda_i v_{ir} y_{ij}^r W_{jr}$ for each priority class.

We generate 10 instances randomly, and similar results are observed from all instances. The results of a typical instance are shown in Table 1. As expected, we see an increasing trend of Z_1 and a decreasing trend of Z_2 as the coefficient w_1 goes down, but the trends are not remarkable. We observe that other measures are also insensitive to w_r except for some extreme parameters, such as $w_1 = 100$. Indeed, the weight of priorities w_r can hardly influence the performance of any priority class in the static system since higher priority demands have already been respected. The performance of class 1 demands usually

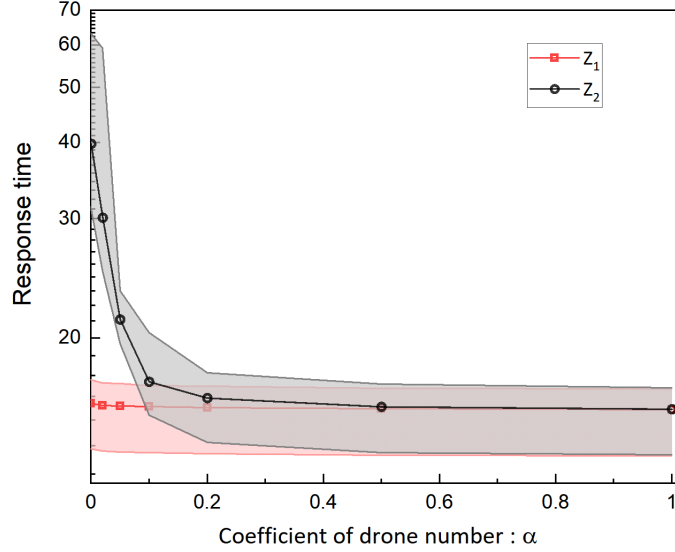


Figure 2 Maximum expected response time of class 1 and class 2 demands with different α (0, 0.02, 0.05, 0.1, 0.2, 0.5, 1)

maintains a steady state, as illustrated in section 6.1.1, it is less affected by the number of drones. However, w_r matters in a dynamic priority system, as we will later see in Table 2.

Table 1 Static-priority system performance by varying w_1 with $\alpha = 0.1, 0.2,$ and 0.5

α	$w_1(\%)$	Response time		Total response time		Waiting time		Total waiting time	
		Z_1	Z_2	$sumZ_1$	$sumZ_2$	W_1	W_2	$sumW_1$	$sumW_2$
0.1	100	11.185	15.882	34.403	52.874	0.603	6.882	1.903	20.374
	99	11.243	15.882	34.178	54.199	0.468	6.882	1.678	21.699
	70	11.269	14.647	34.149	51.475	0.468	6.647	1.649	18.975
	50	11.269	14.647	34.149	51.475	0.468	6.647	1.649	18.975
	30	11.269	14.647	34.149	51.475	0.468	6.647	1.649	18.975
	10	11.269	14.647	34.149	51.475	0.468	6.647	1.649	18.975
	0	11.269	14.647	34.149	51.475	0.468	6.647	1.649	18.975
	0.2	100	11.110	15.882	34.291	52.094	0.603	6.882	1.791
99		11.155	13.405	34.082	44.721	0.477	5.405	1.582	12.221
70		11.185	11.738	33.935	41.275	0.394	2.974	1.335	9.775
50		11.185	11.738	33.935	41.275	0.394	2.974	1.335	9.775
30		11.185	11.738	33.935	41.275	0.394	2.974	1.335	9.775
10		11.185	11.738	33.935	41.275	0.394	2.974	1.335	9.775
0		11.185	11.738	33.935	41.275	0.394	2.974	1.335	9.775
0.5		100	11.033	25.071	33.879	63.587	0.430	12.071	1.379
	99	11.053	11.084	33.598	40.377	0.350	2.974	1.098	7.877
	70	11.053	11.084	33.598	40.377	0.350	2.974	1.098	7.877
	50	11.053	11.084	33.598	40.377	0.350	2.974	1.098	7.877
	30	11.053	11.084	33.598	40.377	0.350	2.974	1.098	7.877
	10	11.053	11.084	33.598	40.377	0.350	2.974	1.098	7.877
	0	16.521	11.057	36.326	40.349	3.521	2.974	2.826	7.849

In order to reveal the relative changes of the two priority demands more intuitively, we use Figure 3 to display the ratio of the total response time and waiting time of class 1 to class 2 demand by varying w_1 with $\alpha = 0.1, 0.2,$ and 0.5 . It is noted that the total waiting time of class 1 demands is relatively small compared to that of class 2, where the ratio is below 10% with $\alpha = 0.1$ and a little higher with larger α . The decreasing trend of the ratio is not noticeable with w_1 except at the extreme value. The ratio of total response time is larger than that of total waiting time, while the variation trend is similar. Overall, the weight coefficient w_r has less impact on the response time and waiting time of both classes, reflecting the nature of static priority.

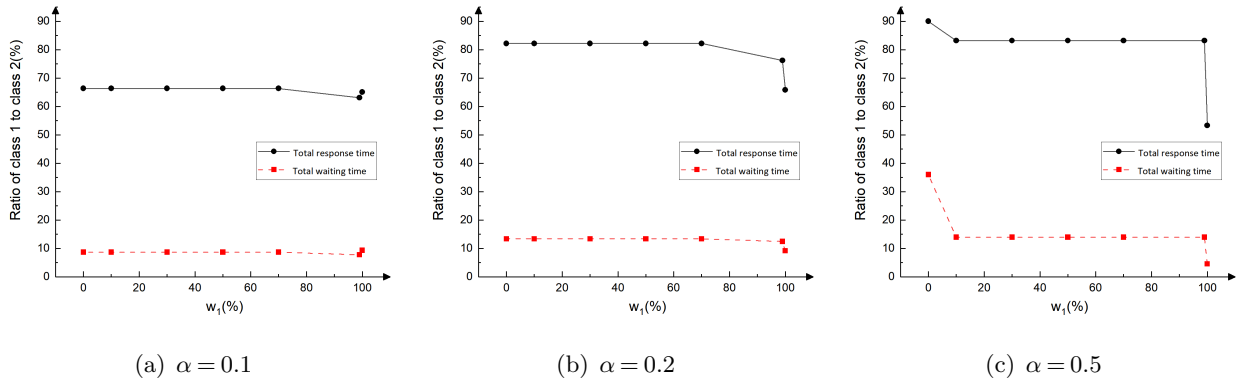


Figure 3 Ratio of total response time and total waiting time of class 1 to class 2 demand by varying w_1 with $\alpha = 0.1, 0.2,$ and 0.5

6.1.3. Comparison with the non-priority system

In this section, we compare the performance of our congested facility location-allocation system with static priority to that with non-priority. Each demand is given the same priority class in the non-priority system as in the static priority system so as to get the same objective function. Figure 4 presents the box plots of the gap of total response time and waiting time between the static priority system and non-priority system, which is calculated as follows:

$$Gap = \frac{T_{SP} - T_{NP}}{T_{NP}} \times 100\%,$$

where T_{SP} represents the total response time or waiting time in the static priority system and T_{NP} for that in the non-priority system. 20 instances are randomly generated with the parameter setting $\alpha = 0.1$ and $w_1 = 70\%$.

According to the negative values of Gap for total response time and total waiting time of class 1 demand and the positive values of class 2 demands, we can conclude that introducing static priority discipline into the delivery system can help decrease both the response time and waiting time of the higher priority demands but incur extra time for lower priority demands. Therefore, when there are demands of urgent need while others are not that emergent, it is more reasonable to apply the static priority. It is also worth mentioning that the gap in waiting time is more substantial than that in response time, the mean absolute value of which are about 15% and 70% respectively. This manifests that although static priority discipline has a considerable impact on waiting time, travel time also accounts for an essential part of the final response time.

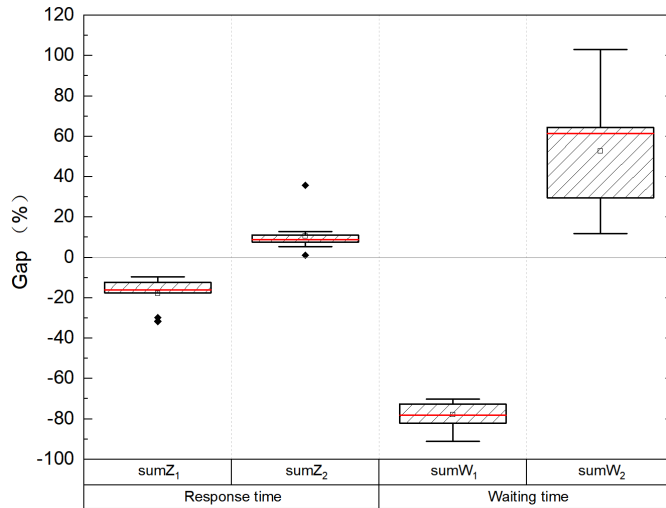


Figure 4 Gap of total response time and total waiting time between the static priority system and non-priority system ($\alpha = 0.1$)

6.2. Analysis of dynamic priority problem

In this section, we present the computational results of our congested facility location-allocation problem with dynamic priority. We investigate the impact of the total number of drones on the system performance under different settings of initial priority-class gap Δa_{ij} . We also conduct an analysis of the weight coefficient w_r in the (DP). The performance of the dynamic system is compared with that of static priority and non-priority queuing-location system.

The instances are random generated with 11 demand nodes and 6 candidate service centers with the distribution mentioned before. Two priority classes are considered. We

randomly choose 6 demand nodes as class 1 demands, and the others belong to class 2. The average arrival rate at demand node i is randomly generated as $\lambda_i \sim U(0.1, 0.5)$. The number of drones used in the system is limited to 200. Since only two priority classes are studied, we use Δa instead of Δa_{12} for simplicity.

6.2.1. Impact of the number of drones

In this section, we exam the impact of the number of drones on the response time for the dynamic priority system. The side model is solved first to get the minimum number of drones K^* . Then (DP) is solved to optimality with different number of drones by varying coefficient $\alpha \in \{0, 0.02, 0.05, 0.1, 0.2, 0.5, 1\}$ under different initial priority-class gap $\Delta a \in \{3, 10, 20\}$. The impacts on the response time are analyzed through the simulation process with respect to the optimal results from (DP) .

Figure 5 represents the results of a typical instance of both the optimization model and the simulation, which illustrates the impact of the total number of drones on the weighted expected response time Z with different Δa . The decreasing trends of Z under all settings of Δa in both situations (optimization and simulation) are similar to those in the static priority queuing system, which fall rapidly at the beginning and then become stable till the end. This result also implies that it is appropriate to deploy drones with α around 0.2 in the whole system. Since the upper bound is used in the optimization model of the dynamic problems, the value of Z is slightly higher than that obtained from the simulation. Besides, we find that the curves with larger Δa lie above or align with those with smaller Δa . This observation indicates that a larger initial priority gap between two classes will lead to a larger weighted expected response time in general. All the three lines converge to a certain value as α approaches 1, which is associated with the fact that the waiting time is extremely small and only travel time matters for the response time when drones are exceedingly sufficient.

The changes in Z_r , which is the expected maximum response time of class r demands by varying coefficient α of drone number when $\Delta a = 3, 10$ and 20 can be seen in Figure 6. 10 instances are randomly developed for each setting. The mean values, the upper and the lower quartiles of Z_r are displayed in the graphs. As expected, the response times of both classes decline as the number of drones increases and finally converge to a certain value in all settings. Besides, with the growth of Δa , the downward trend of Z_1 becomes flatter, indicating the declining influence of α on the response time of high priority demands. While

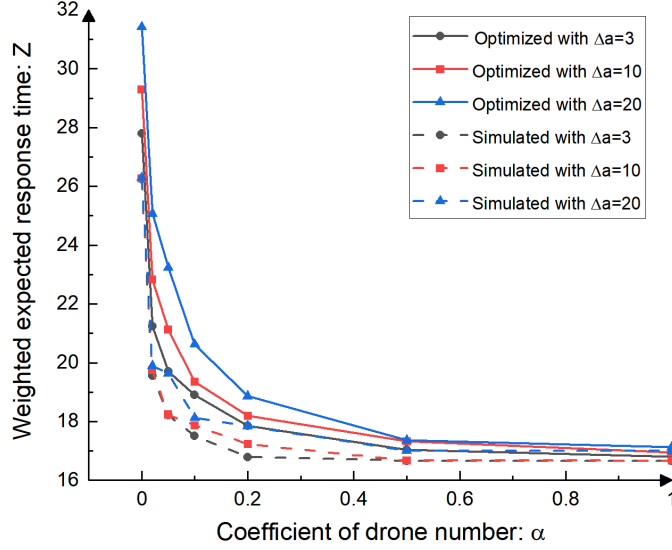


Figure 5 The impact of total number of drones on the weighted expected response time Z with different Δa (3, 10, 20)

the gap between Z_1 and Z_2 becomes larger as Δa grows. In order to show this phenomenon more directly, we present the ratio of Z_2/Z_1 of a typical instance in Figure 7. The ratio with a larger Δa is always higher than that of a smaller value. The lower the ratio, the smaller the difference between the two classes. As Δa increases, the initial priority value plays a more prominent role than time in the final priority value, leading to a larger gap of the response time between the two classes, which approaches the situation in the static system.

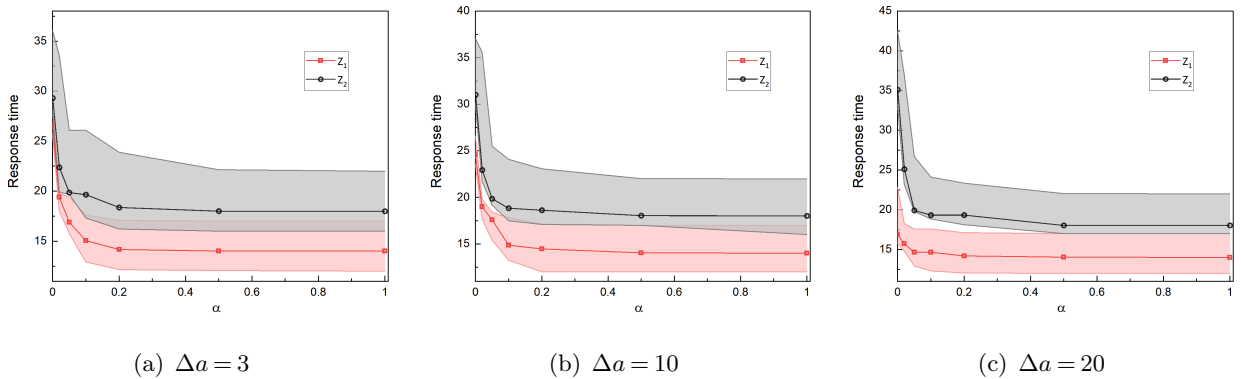


Figure 6 Maximum expected response time of class 1 and class 2 demands with different α ($\Delta a = 3, 10, \text{and } 20$)

6.2.2. Impact of the weight coefficients

In this section, we study the impact of the weight of priorities w_r on the maximum

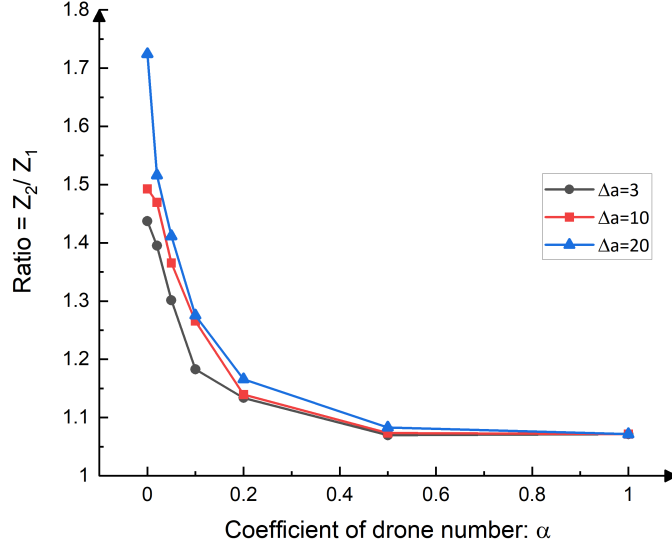


Figure 7 Ratio of the maximum expected response time of class 1 demand to class 2 demand

response time Z_r , the total response time $sumZ_r = \sum_{i \in I_r} \lambda_i y_{ij} (t_{ij} + W_{jr})$, the maximum waiting time W_r , and the total waiting time $sumW_r = \sum_{i \in I_r} \lambda_i y_{ij} W_{jr}$.

In Table 2, we report the results of a typical instance with $\Delta a = 3, 10$, and 20 and $\alpha = 0.1, 0.2$, and 0.5. Similar to the results in the static priority system, the response time of class 2 changes in the same direction as w_1 , while class 1 is the opposite. The trends of $sumZ_r$, W_r , and $sumW_r$ correspond to Z_r in general except for some extreme values. Overall, the values of all indicators tend to be improved with the rise of α consistent with the conclusions in section 6.2.1.

To show the impact of w_r on each priority class more intuitively, we display the ratios of total waiting time and total response time of class 1 versus class 2 with $\alpha = 0.1$ in Figure 8. The growth of w_1 leads to a decreasing trend in the ratio of both waiting time and response time. This effect is especially pronounced with smaller Δa where the preferential treatment of class 1 demand is not that strict. We observe that the ratio of the total response time is larger with smaller Δa generally, so is the total waiting time. This can be explained that larger Δa means more significant priority-class differences, where class 1 demand is more prioritized, yielding a larger gap between the two classes. Overall, the weight coefficients have a great impact with small Δa and a slight impact with large Δa on the system performance. We can adjust the importance of each priority class by using different w_r in dynamic priority system to match the actual situation.

Table 2 System performance by varying w_1 with $\alpha = 0.1, 0.2, 0.5$ and $\Delta a = 3, 10, 20$

Δa	α	$w_1(\%)$	Response time		Total response time		Waiting time		Total waiting time	
			Z_1	Z_2	$sumZ_1$	$sumZ_2$	W_1	W_2	$sumW_1$	$sumW_2$
3	0.1	100	14.446	21.476	18.000	24.011	3.300	9.911	4.609	12.684
		70	14.943	17.678	16.709	18.453	2.009	3.753	1.462	2.678
		50	14.943	17.678	16.709	18.453	2.009	3.753	1.462	2.678
		30	16.467	16.130	17.943	17.244	3.243	2.544	2.467	3.960
		0	16.467	16.130	17.943	17.244	3.243	2.544	2.467	3.960
3	0.2	100	14.066	21.476	17.544	23.775	2.844	9.675	4.609	12.684
		70	14.228	16.856	15.539	16.203	0.839	2.103	0.941	1.856
		50	14.446	15.578	16.053	16.162	1.353	2.062	1.363	2.394
		30	14.943	15.235	16.650	16.218	1.950	2.118	1.363	2.394
		0	16.467	15.097	18.478	16.783	3.778	2.683	2.467	3.960
3	0.5	100	14.000	21.476	17.465	23.733	2.765	9.633	4.609	12.684
		70	14.010	15.038	15.530	15.564	0.830	1.464	1.363	2.394
		50	14.035	15.011	15.077	15.861	0.377	1.161	0.557	1.262
		30	14.122	15.001	15.080	14.671	0.380	0.571	0.389	0.820
		0	14.943	15.000	16.066	15.132	1.366	1.032	0.943	1.800
10	0.1	100	14.370	21.950	16.770	24.546	2.070	10.446	2.711	12.684
		70	14.764	18.684	15.892	20.493	1.192	6.393	0.764	12.684
		50	14.764	18.684	15.892	20.493	1.192	6.393	0.764	12.684
		30	14.764	18.684	15.892	20.493	1.192	6.393	0.764	12.684
		0	16.077	16.557	17.650	18.402	2.950	4.302	2.077	5.878
10	0.2	100	14.060	21.950	16.399	24.209	1.699	10.109	2.711	12.684
		70	14.201	16.557	15.398	16.822	0.698	2.722	0.762	2.674
		50	14.370	15.578	15.601	16.437	0.901	2.337	0.762	2.674
		30	14.764	15.578	15.791	15.773	1.091	1.673	0.764	2.679
		0	14.764	15.295	15.675	15.858	0.975	1.158	0.764	2.679
10	0.5	100	14.000	21.950	16.327	24.160	1.627	10.060	2.711	12.684
		70	14.037	15.038	17.114	14.672	0.514	3.572	0.350	0.872
		50	14.060	15.005	14.947	14.675	0.247	0.575	0.291	0.872
		30	14.060	15.005	14.947	14.675	0.247	0.575	0.291	0.872
		0	14.370	15.000	15.253	15.586	0.553	0.886	0.370	1.287
20	0.1	100	14.344	22.209	16.085	24.818	1.385	10.718	1.621	12.684
		70	14.649	18.684	15.718	20.680	1.018	6.580	0.649	12.684
		50	14.649	18.684	15.718	20.680	1.018	6.580	0.649	12.684
		30	14.649	18.684	15.718	20.680	1.018	6.580	0.649	12.684
		0	14.649	17.889	15.728	19.144	1.028	4.444	0.649	3.257
20	0.2	100	14.060	22.209	15.744	24.443	1.044	10.343	1.621	12.684
		70	14.195	16.174	15.089	16.301	0.389	1.601	0.259	1.174
		50	14.195	16.174	15.089	16.301	0.389	1.601	0.259	1.174
		30	14.195	16.174	15.089	16.301	0.389	1.601	0.259	1.174
		0	14.649	15.295	15.537	16.031	0.837	1.331	0.649	3.257
20	0.5	100	14.000	17.889	14.950	18.167	0.250	3.467	0.416	2.889
		70	14.018	15.183	18.123	14.931	1.623	0.231	2.669	0.183
		50	14.034	15.097	16.077	14.272	1.377	0.172	4.350	0.149
		30	14.034	15.092	19.437	14.835	2.937	0.135	4.350	0.092
		0	14.344	15.000	15.286	15.048	0.586	0.948	0.344	1.416

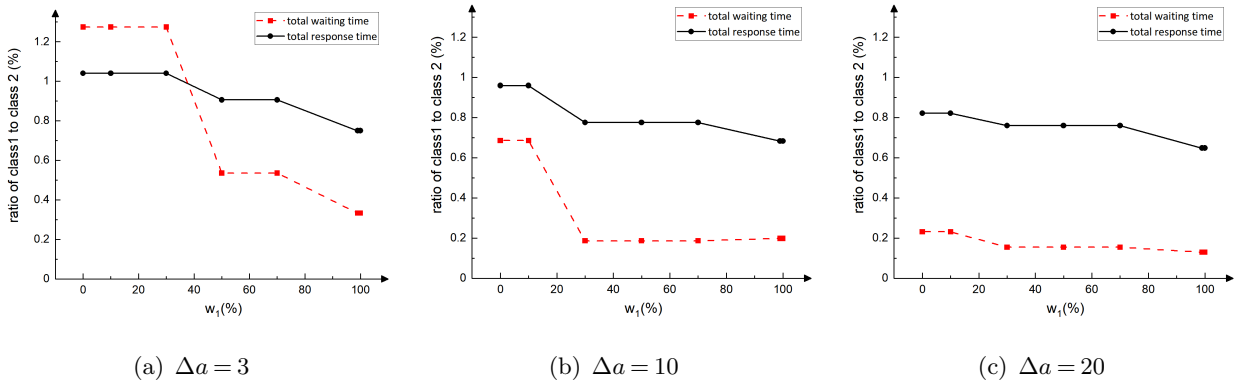


Figure 8 Ratio of total response time and total waiting time of class 1 to class 2 demand by varying w_1 with $\alpha = 0.1$

6.2.3. Comparison of the three priority systems

In this section, the comparisons of performance among dynamic priority, static priority, and non-priority systems are provided. The priority class of each demand node and the objective are the same under the three priority disciplines. All experiments are performed with $\alpha = 0.1$. We use DP for dynamic problem, SP for static problem, and NP for non-priority problem for simplicity.

The box plot in Figure 9 displays the gap of the maximum expected response and waiting time between the dynamic priority system and the static priority or non-priority system, which takes the value

$$Gap = \frac{T_{DP} - T_{SP}(T_{NP})}{T_{SP}(T_{NP})} \times 100\%,$$

where T_{DP} represents the response or waiting time in the dynamic priority system, T_{NP} and T_{SP} indicate those in the non-priority and static priority systems. 20 instances are randomly generated under each setting. Compared to NP, DP sees lower response and waiting time for class 1 demands and higher values for class 2 demands, which is also the case when comparing SP with NP (see section 6.1.3). However, when DP is compared to SP (see the red boxes in the figure), the trend is completely the opposite. This agrees with the intuition that when compared with a static priority system, dynamic priority discipline reduces precedence of class 1 demands, leading to a longer waiting time of class 1 and a shorter waiting time of class 2. However, the opposite effect happens when compared with a non-priority system.

Actually, the congested facility location-allocation system with static priority and without priority are two special cases of the system with dynamic priority when Δa is set to

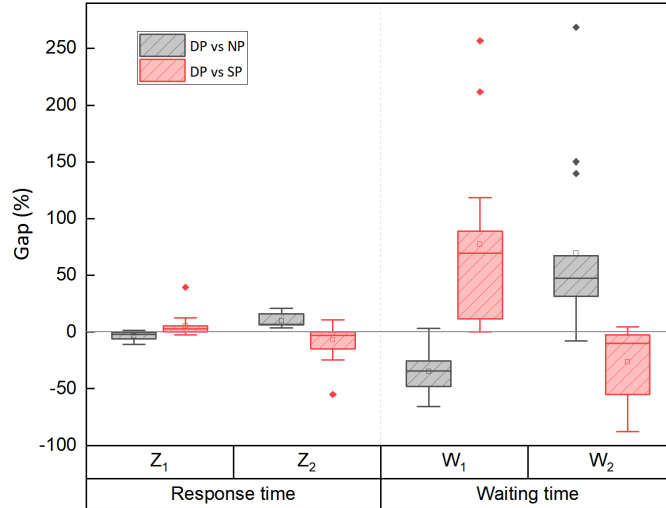


Figure 9 Gap of maximum response and waiting time between the dynamic priority system and the static priority or non-priority system with $\Delta a = 3$

$+\infty$ and 0 respectively. The results in Figure 10 support this point: the gap of the response time between the two classes equals 0 when $\Delta a = 0$ compared with non-priority system and gradually approaches 0 as Δa becomes extremely large compared with the static priority system.

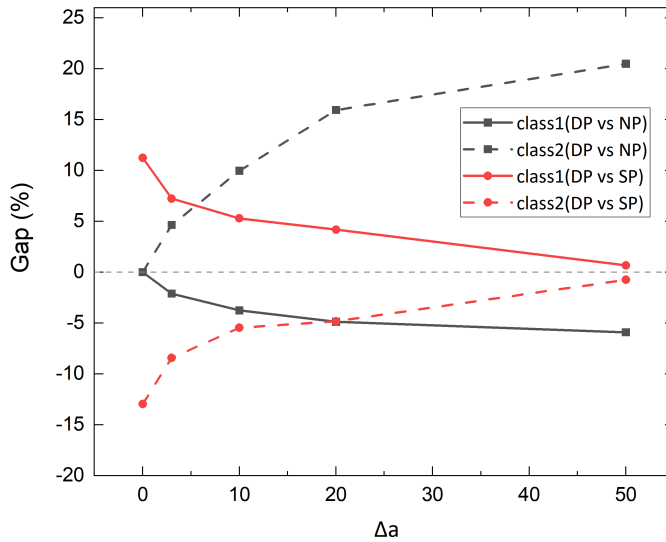


Figure 10 Gap of maximum response time between the dynamic priority system and the static priority or non-priority system by varying Δa

In addition to the overall value of system performance, we further investigate the waiting time of each individual in our emergency delivery system. The waiting time of each demand with priority r is collected through the simulation process, denoted by w_r . Tail probability

is introduced, which indicates the probability of w_r larger than some tail value t , that is $P(w_r > t)$. Figure 11 displays the changes of the tail probability of waiting time as t increases for the two priority classes in the dynamic and static systems with $\Delta a = 3$, $\alpha = 0.1$. We observe the decreasing monotonicity in all the four groups, and the tail probability of class 1 demand from the static priority system declines faster than that from the dynamic priority system, while the opposite is the case for class 2 demand. The strict priority discipline in the static priority system leads to the excessive waiting time of some class 2 demands. As can be seen, about 20 percent of demands need to wait for more than 10 time units. This observation suggests that dynamic priority can effectively eliminate the extremely long waiting time of the lower priority class when adopting the priority mechanism.

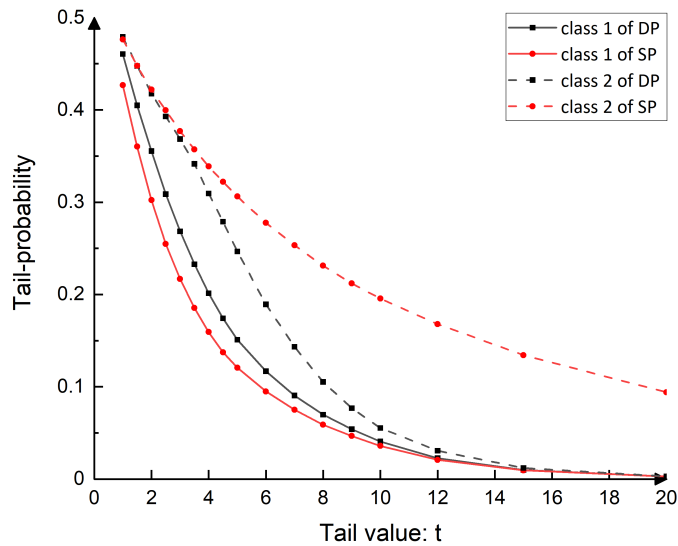


Figure 11 Tail probability $P(W_r > t)$

7. Conclusions and future work

In this paper, the queuing-location models with three priority disciplines are proposed, which are FCFS, static priority, and dynamic priority. The optimal decisions of the facility location, demand allocation, and deployment of drones are made simultaneously. In the model, drones are regarded as mobile servers with a general service time related to the allocation and capacity decisions. The worst expected response time among all demands is minimized in our problem concerning the equity of the emergency service. According to the

nonlinear nature of the proposed models, we reformulate the original models into mixed-integer second-order cone programs that can be solved with computational efficiency.

The optimal decisions from the mathematical models are input to the simulation to conduct the sensitivity analysis and evaluate the system performance. The observation from the results suggests the unnecessary to distribute excessive drones at a higher cost. According to the instances analyzed in this study, it is recommended to set the number of drones with α around 0.2. The weight coefficient of the priority in the static priority system is ineffective to adjust the importance of the priority classes, but it works in the dynamic system, especially under a small initial priority-class gap. The results also show the necessity to apply suitable priority disciplines for different situations to improve the system performance and provide better service. Static priority discipline is more suitable when there are demands of a particularly urgent need, since it can significantly reduce the response time of the high priority demands. Dynamic priority can effectively eliminate the extremely long waiting time of the lower priority class when adopting the priority mechanism. Therefore, the impact of the dynamic priority lies between the static priority and non-priority disciplines, and can be adjusted by the initial priority-class gap.

When dealing with the dynamic priority system, the upper bound of the waiting time is used, leading to the non-optimality of the final results in several instances. Our future research will try to use the exact value of waiting time in the facility location-allocation problem with dynamic priority. Besides, inseparable demands are assumed in our problem, where each demand can only be assigned to exactly one facility. In the future, we can consider separable demands and allow them to be allocated to several different facilities. Another interesting and useful research direction is to extend the problem to robust or stochastic programming models to address the uncertainty factors such as the travel time or user demands.

References

- 2015 *Classification catalog of key emergency supplies (in chinese)*. Technical report, National Development and Reform Commission.
- Aboolian R, Berman O, Drezner Z, 2009 *The multiple server center location problem*. *Annals of Operations Research* 167(1):337–352.
- Agatz N, Bouman P, Schmidt M, 2018 *Optimization approaches for the traveling salesman problem with drone*. *Transportation Science* 52(4):965–981.

- Ahmadi-Javid A, Berman O, Hoseinpour P, 2018 *Location and capacity planning of facilities with general service-time distributions using conic optimization*. *arXiv preprint arXiv:1809.00080* .
- Ahmadi-Javid A, Hoseinpour P, 2017 *Convexification of queueing formulas by mixed-integer second-order cone programming: an application to a discrete location problem with congestion*. *arXiv preprint arXiv:1710.05794* .
- Ahmadi-Javid A, Ramshe N, 2019 *Linear formulations and valid inequalities for a classic location problem with congestion: a robust optimization application*. *Optimization Letters* 1–21.
- Bagchi U, Sullivan RS, 1985 *Dynamic, non-preemptive priority queues with general, linearly increasing priority function*. *Operations research* 33(6):1278–1298.
- BAKER A, 2017 *The american drones saving lives in rwanda*. *TIME* <https://time.com/rwanda-drones-zipline/>.
- Batta R, Berman O, 1989 *A location model for a facility operating as an m/g/k queue*. *Networks* 19(6):717–728.
- Batta R, Dolan JM, Krishnamurthy NN, 1989 *The maximal expected covering location problem: Revisited*. *Transportation science* 23(4):277–287.
- Berman O, Krass D, 2019 *Stochastic location models with congestion*. *Location science*, 477–535 (Springer).
- Berman O, Krass D, Wang J, 2006 *Locating service facilities to reduce lost demand*. *IIE Transactions* 38(11):933–946.
- Berman O, Larson RC, Chiu SS, 1985 *Optimal server location on a network operating as an m/g/1 queue*. *Operations research* 33(4):746–771.
- Berman O, Larson RC, Parkan C, 1987 *The stochastic queue p-median problem*. *Transportation Science* 21(3):207–216.
- Berman O, Mandowsky RR, 1986 *Location-allocation on congested networks*. *European Journal of Operational Research* 26(2):238–250.
- Boutillier JJ, Chan TC, 2019 *Response time optimization for drone-delivered automated external defibrillators*. *arXiv preprint arXiv:1908.00149* .
- Cao Ls, Liu Zx, 2011 *An emergency service center location model for vehicle repair with priority queueing rules and service level constraints*. *2011 IEEE 18th International Conference on Industrial Engineering and Engineering Management*, 1333–1336 (IEEE).
- Chiu SS, Berman O, Larson RC, 1985 *Locating a mobile server queueing facility on a tree network*. *Management Science* 31(6):764–772.
- Chung SH, Sah B, Lee J, 2020 *Optimization for drone and drone-truck combined operations: A review of the state of the art and future directions*. *Computers & Operations Research* 105004.

- COMMUNITY W, 25th April 2020 *How delivery drones are being used to tackle covid-19 (updated)*. *WeRobotics* <https://blog.werobotics.org/2020/04/25/cargo-drones-covid-19/>.
- Daknama R, Kraus E, 2017 *Vehicle routing with drones*. *arXiv preprint arXiv:1705.06431* .
- Dan T, Marcotte P, 2019 *Competitive facility location with selfish users and queues*. *Operations Research* 67(2):479–497.
- Daskin MS, 1983 *A maximum expected covering location model: formulation, properties and heuristic solution*. *Transportation science* 17(1):48–70.
- Elhedhli S, 2006 *Service system design with immobile servers, stochastic demand, and congestion*. *Manufacturing & Service Operations Management* 8(1):92–97.
- Ferrandez SM, Harbison T, Weber T, Sturges R, Rich R, 2016 *Optimization of a truck-drone in tandem delivery network using k-means and genetic algorithm*. *Journal of Industrial Engineering and Management (JIEM)* 9(2):374–388.
- Fujiwara O, Makjamroen T, Gupta KK, 1987 *Ambulance deployment analysis: A case study of bangkok*. *European Journal of Operational Research* 31(1):9–18.
- Ghannadpour SF, Noori S, Tavakkoli-Moghaddam R, 2014 *A multi-objective vehicle routing and scheduling problem with uncertainty in customers' request and priority*. *Journal of Combinatorial Optimization* 28(2):414–446.
- Goldberg J, Dietrich R, Chen JM, Mitwasi MG, Valenzuela T, Criss E, 1990 *Validating and applying a model for locating emergency medical vehicles in tucson, az*. *European Journal of Operational Research* 49(3):308–324.
- Ha QM, Deville Y, Pham QD, Ha MH, 2018 *On the min-cost traveling salesman problem with drone*. *Transportation Research Part C: Emerging Technologies* 86:597–621.
- Harewood S, 2002 *Emergency ambulance deployment in barbados: a multi-objective approach*. *Journal of the Operational Research Society* 53(2):185–192.
- Jackson JR, 1960 *Some problems in queueing with dynamic priorities*. *Naval Research Logistics Quarterly* 7(3):235–249.
- Jackson JR, 1961 *Queues with dynamic priority discipline*. *Management Science* 8(1):18–34.
- Jayaswal S, Vidyarthi N, 2017 *Facility location under service level constraints for heterogeneous customers*. *Annals of Operations Research* 253(1):275–305.
- Jia H, Ordóñez F, Dessouky M, 2007 *A modeling framework for facility location of medical services for large-scale emergencies*. *IIE transactions* 39(1):41–55.
- Kitjacharoenchai P, Min BC, Lee S, 2020 *Two echelon vehicle routing problem with drones in last mile delivery*. *International Journal of Production Economics* 225:107598.

- Li W, Wu Z, Song L, 2018 *Single-level lrp problem of emergency logistics system considering demand priority. E&ES* 189(6):062020.
- Macrina G, Pugliese LDP, Guerriero F, Laporte G, 2020 *Drone-aided routing: A literature review. Transportation Research Part C: Emerging Technologies* 120:102762.
- Marianov V, ReVelle C, 1994 *The queuing probabilistic location set covering problem and some extensions. Socio-Economic Planning Sciences* 28(3):167–178.
- Marianov V, ReVelle C, 1996 *The queueing maximal availability location problem: a model for the siting of emergency vehicles. European Journal of Operational Research* 93(1):110–120.
- Marianov V, Serra D, 1998 *Probabilistic, maximal covering location—allocation models for congested systems. Journal of Regional Science* 38(3):401–424.
- Marianov V, Serra D, 2002 *Location–allocation of multiple-server service centers with constrained queues or waiting times. Annals of Operations Research* 111(1-4):35–50.
- Max Roser EOO Hannah Ritchie, Hasell J, 2021 *Coronavirus pandemic (covid-19). Our World in Data* <https://ourworldindata.org/coronavirus>.
- McNabb M, 2020 *Drone delivery for coronavirus: Drone delivers test samples to lab in 7 minutes. WeRobotics* <https://dronelife.com/2020/06/04/drone-delivery-for-coronavirus-in-germany/>.
- Mukhopadhyay A, Vorobeychik Y, 2017 *Prioritized allocation of emergency responders based on a continuous-time incident prediction model. International Conference on Autonomous Agents and MultiAgent Systems*.
- Murray CC, Chu AG, 2015 *The flying sidekick traveling salesman problem: Optimization of drone-assisted parcel delivery. Transportation Research Part C: Emerging Technologies* 54:86–109.
- Oran A, Tan KC, Ooi BH, Sim M, Jaillet P, 2012 *Location and routing models for emergency response plans with priorities. Future Security Research Conference*, 129–140 (Springer).
- Otto A, Agatz N, Campbell J, Golden B, Pesch E, 2018 *Optimization approaches for civil applications of unmanned aerial vehicles (uavs) or aerial drones: A survey. Networks* 72(4):411–458.
- Poikonen S, Golden B, Wasil EA, 2019 *A branch-and-bound approach to the traveling salesman problem with a drone. INFORMS Journal on Computing* 31(2):335–346.
- Poikonen S, Wang X, Golden B, 2017 *The vehicle routing problem with drones: Extended models and connections. Networks* 70(1):34–43.
- Repede JF, Bernardo JJ, 1994 *Developing and validating a decision support system for locating emergency medical vehicles in louisville, kentucky. European journal of operational research* 75(3):567–581.
- ReVelle C, Hogan K, 1988 *A reliability-constrained siting model with local estimates of busy fractions. Environment and Planning B: Planning and Design* 15(2):143–152.
- ReVelle C, Hogan K, 1989 *The maximum availability location problem. Transportation science* 23(3):192–200.

- Revelle C, Hogan K, 1989 *The maximum reliability location problem and α -reliable-center problem: Derivatives of the probabilistic location set covering problem*. *Annals of Operations Research* 18(1):155–173.
- Ritchie H, 2014 *Natural disasters*. *Our World in Data* <https://ourworldindata.org/natural-disasters>.
- Salama M, Srinivas S, 2020 *Joint optimization of customer location clustering and drone-based routing for last-mile deliveries*. *Transportation Research Part C: Emerging Technologies* 114:620–642.
- Scott J, Scott C, 2017 *Drone delivery models for healthcare*. *Proceedings of the 50th Hawaii international conference on system sciences*.
- Shavarani SM, 2019 *Multi-level facility location-allocation problem for post-disaster humanitarian relief distribution*. *Journal of Humanitarian Logistics and Supply Chain Management* .
- Shavarani SM, Mosallaeipour S, Golabi M, İzbirak G, 2019 *A congested capacitated multi-level fuzzy facility location problem: An efficient drone delivery system*. *Computers & Operations Research* 108:57–68.
- Shortle JF, Thompson JM, Gross D, Harris CM, 2018 *Chapter 4.4 priority queue disciplines*. *Fundamentals of queueing theory* (John Wiley & Sons).
- Silva F, Serra D, 2008 *Locating emergency services with different priorities: the priority queuing covering location problem*. *Journal of the Operational Research Society* 59(9):1229–1238.
- Tian Z, 2016 *Research on the Resources Allocation Problem Considering Priority and Uncertainty in Emergency Dispatch System*. Master's thesis, Chang'an University, China.
- Tijms HC, Van Hoorn MH, Federgruen A, 1981 *Approximations for the steady-state probabilities in the M/G/c queue*. *Advances in Applied Probability* 13(1):186–206.
- Vidyarthi N, Jayaswal S, 2014 *Efficient solution of a class of location-allocation problems with stochastic demand and congestion*. *Computers & Operations Research* 48:20–30.
- Wang Q, Batta R, Rump CM, 2002 *Algorithms for a facility location problem with stochastic customer demand and immobile servers*. *Annals of operations Research* 111(1-4):17–34.
- Wang X, Poikonen S, Golden B, 2017 *The vehicle routing problem with drones: Several worst-case results*. *Optimization Letters* 11(4):679–697.
- Wang Z, Sheu JB, 2019 *Vehicle routing problem with drones*. *Transportation research part B: methodological* 122:350–364.
- Zhu L, Gong Y, Xu Y, Gu J, 2019 *Emergency relief routing models for injured victims considering equity and priority*. *Annals of Operations Research* 283(1-2):1573–1606.